

# Hole stripe and orbital fluctuating state in $\text{LaMnO}_{3+\delta}$ ( $0.085 \leq \delta \leq 0.125$ ) unveiled by Raman spectroscopy

Yu. G. Pashkevich,<sup>1</sup> V. P. Gnezdilov,<sup>2</sup> P. Lemmens,<sup>3</sup> K.-Y. Choi,<sup>4,†</sup> G. Güntherodt,<sup>5</sup> A. V. Eremenko,<sup>2</sup> D. Nabok,<sup>1</sup> V. I. Kamenev,<sup>1</sup> S. N. Barilo,<sup>6</sup> S. V. Shiryayev,<sup>6</sup> and A. G. Soldatov<sup>6</sup>

<sup>1</sup> A. A. Galkin Donetsk Phystech NASU, 83114 Donetsk, Ukraine

<sup>2</sup> B. I. Verkin Institute for Low Temperature Physics NASU, 61164 Kharkov, Ukraine

<sup>3</sup> Institute for Physics of Condensed Matter, TU Braunschweig, D-38106 Braunschweig, Germany

<sup>4</sup> Institute for Materials Research, Tohoku University, Katahira 2-1-1, Sendai 980-8577, Japan

<sup>5</sup> 2. Physikalisches Institut, RWTH Aachen, 52056 Aachen, Germany and

<sup>6</sup> Institute of Physics of Solids & Semiconductors, Academy of Sciences, 220072 Minsk, Belarus

(Dated: December 20, 2018)

Giant softening by  $30 \text{ cm}^{-1}$  of the 490- and  $620\text{-cm}^{-1}$  modes is observed by Raman scattering measurements below the Curie temperature of single crystalline  $\text{LaMnO}_{3+\delta}$  ( $0.085 \leq \delta \leq 0.125$ ). A pseudogap-like electronic continuum and a Fano antiresonance at  $144 \text{ cm}^{-1}$  appear below the charge ordering temperature. This gives evidence for the presence of an orbital fluctuating state and the formation of a hole stripe, respectively. This is further corroborated by a unstructured broadening and shifting of multiphonon features with increasing doping  $\delta$ . Our study suggests the significance of double exchange mechanism in the charged ordered insulating state.

PACS numbers:

One topical issue in the physics of manganites is on the role of orbital degrees of freedom as well as the state of an orbital subsystem at different doping level in explaining a complex phase diagram [1, 2]. The most intriguing feature is found in the low-doped region  $\text{La}_{1-x}\text{Sr}_x\text{MnO}_3$  ( $x = 0.11 - 0.17$ ), which shows the unusual coexistence of ferromagnetism and insulating behavior [3, 4, 5, 6, 7, 8, 9, 10, 11].

To account for the occurrence of a ferromagnetic insulating state several different models have been proposed on the orbital and charge ordering pattern. There is some evidence for a structural modulation with alternating hole-poor and hole-rich planes along the  $c$  axis [6, 7, 12] as well as for a formation of orbital polarons [9, 10, 11, 13]. However, a complete picture is still lacking.

In this paper, we report Raman scattering measurements on the lightly oxygen-doped manganites  $\text{LaMnO}_{3+\delta}$ . We provide evidence for the formation of a hole stripe seen from a pseudogap-like electronic response below the charge ordering temperature. Furthermore, a giant and continuous softening of Mn-O bond stretching modes below the Curie temperature and a unstructured, broadened multiphonon feature suggest a fluctuating orbital state in ferromagnetic samples ( $0.085 \leq \delta \leq 0.125$ ). This together with a Fano antiresonance at  $144 \text{ cm}^{-1}$  signals the significance of double exchange interaction in the ferromagnetic insulating state.

$\text{LaMnO}_{3+\delta}$  single crystals were grown by using a modified method of McCarroll *et al.* [14], which allows for doping without inducing a large cation mass difference. The true crystallographic formula corresponds to  $\text{La}_{1-x}\text{Mn}_{1-y}\text{O}_3$  with  $3/2(x+y) \approx \delta$ . Cation vacancies were controlled by varying the melting temperature. Samples were characterized by X-ray diffraction,

TABLE I: Structural and magnetic properties of  $\text{LaMnO}_{3+\delta}$  with O ( $c \leq b/\sqrt{2} < a$ ) and O' ( $b/\sqrt{2} < c < a$ ) orthorhombic phases with Pnma space group symmetry and R a rhombohedral phase with R $\bar{3}c$  space group symmetry.

sample	magnetic ordering	critical temperature	V/f.u. ( $\text{\AA}^3$ ) T=300 K	crystal structure
3.071	AFM	$T_N=128$ K	59.73	O'
3.085	FM	$T_C=148$ K	59.54	O'
3.092	FM	$T_C=178$ K	59.45	O
3.096	FM	$T_C=186$ K	59.41	O or R
3.125	FM	$T_C=248$ K	59.06	R

magnetic susceptibility and chemical analysis [15]. The structural and magnetic properties are summarized in Table I. Our results are consistent with the previous ones [16, 17]. Furthermore, the magnetic and transport behaviors are quite similar to the lightly-doped  $\text{La}_{1-x}\text{Sr}_x\text{MnO}_3$  ( $0.11 \leq x \leq 0.15$ ) (see Refs. [10, 15]). The slight discrepancy, for example, seen in the irreversible magnetization between field and zero-field cooling should be attributed to additional La-cation disorders.

Raman scattering experiments were performed using the excitation line  $\lambda = 514.5 \text{ nm}$  of an  $\text{Ar}^+$  laser in a quasibackscattering geometry. The laser power of 5 mW was focused to a 0.1 mm diameter spot on the (010) surface. The scattered spectra were collected by a DILOR-XY triple spectrometer and a nitrogen cooled CCD detector with a spectral resolution of  $\sim 1 \text{ cm}^{-1}$ .

Figure 1 displays the doping dependence of polarized Raman spectra of  $\text{LaMnO}_{3+\delta}$  ( $\delta=0.071, 0.085, 0.092, 0.096, \text{ and } 0.125$ ) at 5 and 295 K, respectively. They are compared to the lightly doped manganites

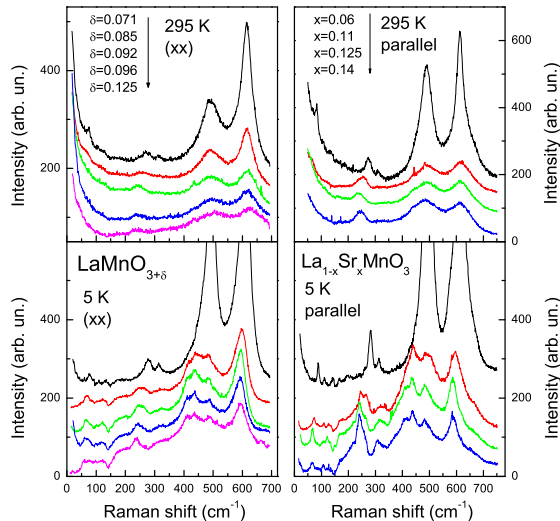


FIG. 1: (online color) (Left panels) Raman spectra of  $\text{LaMnO}_{3+\delta}$  ( $\delta=0.071, 0.085, 0.092, 0.096,$  and  $0.125$ ) in  $(xx)$  polarization as a function of doping at 5 and 295 K, respectively. (Right panels) For comparison, Raman spectra of  $\text{La}_{1-x}\text{Sr}_x\text{MnO}_3$  ( $x=0.06, 0.11, 0.125,$  and  $0.14$ ) are presented together at the respective temperature [11].

$\text{La}_{1-x}\text{Sr}_x\text{MnO}_3$  ( $x=0.06, 0.11, 0.125,$  and  $0.14$ ) that are a counterpart of the title compound [11]. Remarkably, the observed Raman spectra are parallel to each other. For the antiferromagnetic (AF) sample ( $\delta=0.071$  and  $x=0.06$ ) weak peaks arising from vibrations of (La/Sr) cations and rotations of the  $\text{MnO}_6$  octahedra can be resolvable in addition to the three main peaks; the out-of-phase rotational mode around  $250\text{ cm}^{-1}$ , the Jahn-Teller (JT) mode around  $490\text{ cm}^{-1}$ , and the breathing mode around  $620\text{ cm}^{-1}$ . At low temperatures the ferromagnetic insulating (FMI) samples ( $\delta = 0.085 - 0.125$  and  $x = 0.11 - 0.14$ ) show commonly the extra phonon peaks which are split off from the high-temperature modes. This is due to activated modes induced by the charge and orbital ordering. Noticeably, all FMI samples have the identical Raman spectra, irrespective of doping and compound. This implies that all FMI samples are characterized by the same charge and orbital ordering structure in spite of additional, disordered holes as well as of chemical disorders. X-ray measurements of  $\text{La}_{1-x}\text{Sr}_x\text{MnO}_3$  support further this, which exhibits the same superstructure reflections of nearly equal scattering intensity for all  $x$  [5]. This might be related to a robustness of the specific orbital and charge order found at  $x = 1/8$ .

Shown in Figs. 2 is the temperature dependence of the Raman spectra of the representative sample at  $\delta = 0.092$  in  $(xx)$  and  $(x'y')$  polarizations. They exhibit intrigu-

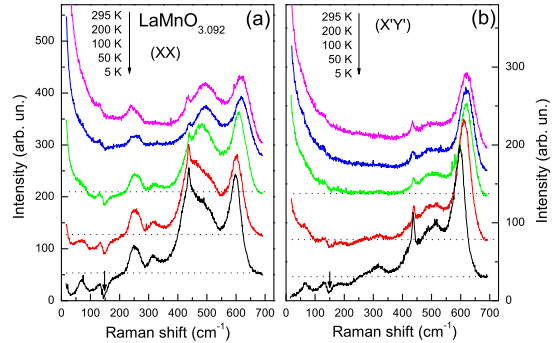


FIG. 2: (color online) Temperature-dependence of Raman spectra of  $\text{LaMnO}_{3+\delta}$  ( $\delta = 0.092$ ) in (a)  $(xx)$  and (b)  $(x'y')$  polarizations. The horizontal dotted lines are a guide for an electronic background. The vertical arrows indicate antiresonance at  $144\text{ cm}^{-1}$ .

ing features. With decreasing temperature the Mn-O stretching modes undergo a large softening in addition to the appearance of new phonon peaks. Furthermore, the low-frequency quasielastic response is systematically suppressed while a pseudogap opens at low temperatures. Noticeably, a strong Fano antiresonance is observed at  $144\text{ cm}^{-1}$  which corresponds to the rotation of the  $\text{MnO}_6$  octahedra.

The most salient feature can be seen in the temperature dependence of the main peaks at  $250, 490,$  and  $620\text{ cm}^{-1}$  as summarized in Fig. 3 as a function of  $\delta$ . The experimental spectra are analyzed by a sum of a Lorentzian profile. Error bars are of the symbol size.

First, let us begin with the out-of-phase rotational mode around  $250\text{ cm}^{-1}$ . This mode is associated with the tolerance factor of the manganites. That is, it provides direct information about octahedral tiltings and Mn-O-Mn bond angles. With increasing  $\delta$  the mode softens by  $40\text{ cm}^{-1}$ . The large doping dependence should be attributed to the suppression of the static JT distortion as hole mobilities increase. This is also reflected in the structural transition from orthorhombic to rhombohedral phase (see Table I). Further, upon cooling the  $250\text{-cm}^{-1}$  mode first hardens up to  $T_C$  and then softens slightly. The magnitude of the hardening decreases as  $\delta$  increases, for example, from  $12\text{ cm}^{-1}$  at  $\delta = 0.085$  to  $4\text{ cm}^{-1}$  at  $\delta = 0.125$ . Here note that between  $T_{JT}$  and  $T_C$  there exists a  $d_{3x^2-r^2}/d_{3y^2-r^2}$  orbital ordering which is similar to that of  $\text{LaMnO}_3$  [9, 10]. This antiferro-orbital ordering is stabilized by the cooperative JT distortion. Therefore, the decrease of the hardening with increasing  $\delta$  further evidences the reduction of the  $\text{LaMnO}_3$ -type orbital order. In this respect, moreover, the softening by  $2\text{-}3\text{ cm}^{-1}$  below  $T_C$  can be interpreted in terms of the fact that the  $\text{LaMnO}_3$ -type orbital above  $T_C$  evolves to the differ-

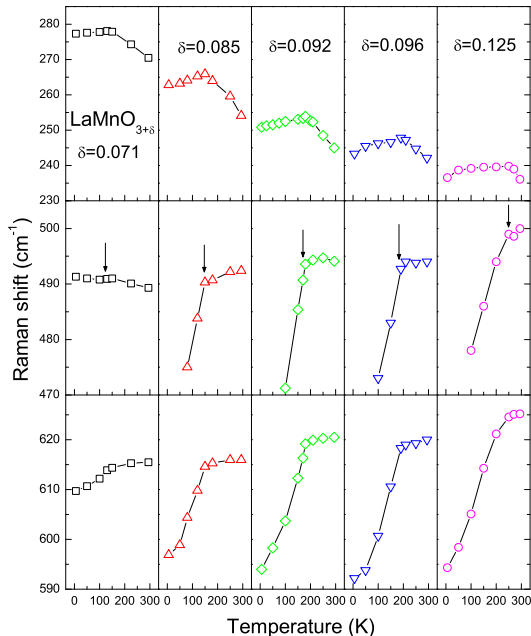


FIG. 3: (color online) Temperature dependence of peak position of the 250-, 490-, and 620-cm<sup>-1</sup> mode as a function of doping  $\delta$ . The vertical arrows indicate the magnetic ordering temperature.

ent type of orbital below  $T_C$ . Actually, resonant X-ray scattering measurements unveil the rearrangement of the orbital ordering through  $T_C$  [9, 10].

Next, we will address the temperature dependence of the  $\text{MnO}_6$  vibrational modes. Upon cooling the JT mode of the AF sample at about 490 cm<sup>-1</sup> shows a slight hardening by 3 cm<sup>-1</sup> while the breathing mode at about 620 cm<sup>-1</sup> undergoes a moderate softening by 6 cm<sup>-1</sup>. For the FMI samples the respective modes turn to a giant softening by 20-30 cm<sup>-1</sup> below  $T_C$ . As  $\delta$  increases, the softening becomes enhanced. Furthermore, the softening does not exhibit any saturation even at very low temperatures. It is worth to note that such a giant softening is exclusively seen at the breathing mode for the lightly doped  $\text{La}_{1-x}\text{Sr}_x\text{MnO}_3$  [11]. This is ascribed to the intrinsic coupling of the breathing mode to orbital polarons and is taken as evidence for the formation of orbital polarons in the hole-rich sites. Most probably, the hole-poor planes are composed of a  $\text{LaMnO}_3$ -type orbital [12]. In this case, the La-site disorder in  $\text{LaMnO}_{3+\delta}$  can lead to the additional softening of the JT-mode in contrast to  $\text{La}_{1-x}\text{Sr}_x\text{MnO}_3$ . Therefore, we conclude that the hole-poor planes contain a  $\text{LaMnO}_3$ -type orbital while the hole-rich planes are dominated by orbital polarons. Moreover, the softening without saturation indicates a fluctuating nature of the underlying orbital state.

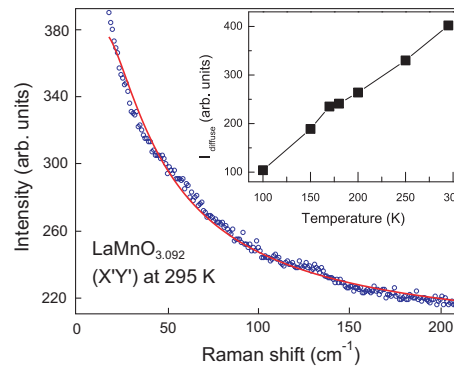


FIG. 4: (color online) A fitting of the low-frequency electronic response of  $\delta = 0.092$  at 295 K using Eq. (1). Inset: Temperature dependence of the scattering amplitude,  $I_{diffuse}$ .

We will now examine the electronic response to get information about hole dynamics. At high temperatures we have observed pronounced quasielastic Raman response. The observed low-frequency response is well described by a diffusive scattering [18];

$$I(\omega, T) = \frac{1}{1 - \exp(\hbar\omega/kT)} \times \frac{I_{diffuse}\omega\Gamma}{\omega^2 + \Gamma^2}, \quad (1)$$

where the first term is the Bose-thermal factor and  $I_{diffuse}$  is the scattering amplitude and  $\Gamma$  the scattering rate. Figure 4 displays the typical fit using Eq. (1) at 295 K. The temperature dependence of the scattering amplitude is shown in the inset of Fig. 4. The scattering rate of  $\Gamma = 13.5 - 14.5$  cm<sup>-1</sup> is nearly temperature independent. Its magnitude is two orders of magnitude smaller than that of the optimal doped  $\text{La}_{1-x}\text{Sr}_x\text{MnO}_3$  [18]. The scattering amplitude of  $I_{diffuse}$  decreases linearly upon cooling. It persists much below the charge ordering temperature,  $T_{CO}$ . The diffusive scattering originates from fluctuations related to electronic scattering from spins and impurities. Therefore, this suggests that holes are not totally frozen-in below  $T_{CO}$ . At low temperatures the depletion of spectral weight is observed below 250 cm<sup>-1</sup> (see Figs. 2). The presence of a pseudogap-like behavior below the charge ordering temperature is due to the formation of a hole stripe as in  $\text{La}_{2-x}\text{Sr}_x\text{NiO}_4$  [19]. Moreover, a Fano antiresonance appears at 144 cm<sup>-1</sup>, pointing to substantial electron-phonon coupling. Here we will remind that a stripe is formed to gain a kinetic energy of holes in the AF background in the cuprates and nickelates. In analogy, a hole stripe in the manganites arises from maximizing locally the gain of double exchange energy while keeping globally an insulating behavior. The evolution of  $\text{LaMnO}_3$ -type orbitals to the new orbital state including orbital polarons through  $T_C$  is also initiated by double-exchange mechanism [10].

Finally, we will turn to the high-frequency Raman spectra of  $\text{LaMnO}_{3+\delta}$  at 5 K which are displayed in Fig.

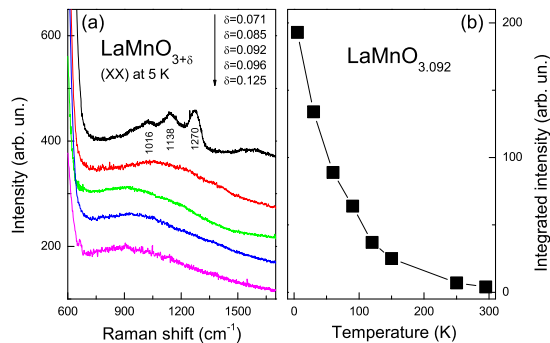


FIG. 5: (a) Raman spectra at  $T=5$  K in the orbiton frequency regime. (b) Temperature evolution of integrated intensity of the maximum at  $900\text{ cm}^{-1}$  in sample M3.

5(a) as a function of  $\delta$ . The AF sample shows similar results as  $\text{La}_{1-x}\text{Sr}_x\text{MnO}_3$  with respect to frequency, number of modes, and temperature dependence [20]. For the FMI sample of  $\delta = 0.085$  the three peaks coalesce into a broad maximum near  $1100\text{ cm}^{-1}$ . Upon further increasing  $\delta$  the broad maximum is shifted to about  $900\text{ cm}^{-1}$ . One-phonon scattering of the  $490$  and  $620\text{ cm}^{-1}$  modes softens by maximum 5% in going from the  $\delta = 0.085$  to  $\delta = 0.125$  sample. In contrast, the spectral weight of the broad maximum softens by 20% for the respective samples. Such a behavior can definitely not be understood within pure multiphonon processes. Note that  $\text{La}_{1-x}\text{Sr}_x\text{MnO}_3$  shows also a broadened maximum around  $1000\text{ cm}^{-1}$  at  $x=0.125$  [20]. This rules out chemical disorders as a plausible origin. The temperature dependence of the integrated intensity of the maximum at  $\delta = 0.092$  is given in Fig. 5(b). With decreasing temperature the intensity exhibits the  $1/T$ -divergence. This suggests that the observed maximum is closely related to the orbital rearrangement through  $T_C$ .

In the AF phase resonant Raman scattering measurements unveiled that multiphonon scattering is governed by resonant process induced by an orbital flip of a  $d_{3x^2-r^2}/d_{3y^2-r^2}$  orbital ordered state [21]. In this situation, a detailed feature of the multi-phonon scattering relies on the underlying orbital ordering pattern. Upon going through the AF/FMI boundary the  $d_{3x^2-r^2}/d_{3y^2-r^2}$  orbitals are rearranged to the alternating orbitals consisting of orbital polarons in the hole-rich planes and a  $d_{3x^2-r^2}/d_{3y^2-r^2}$  orbital in the hole-poor planes. Thus, orbital excitons, which are responsible for the three-peaks

feature in the AF phase, will smear out in the FMI phase. This naturally explains a shift of the multiphonon scattering to lower energy. Further, the unstructured maximum is associated with a fluctuating orbital state. This interpretation of the high-frequency maxima is consistent with the observed giant softening in terms of a mutual coupling between phonons and the orbital fluctuating state.

In summary, our Raman study of the lightly doped manganites  $\text{LaMnO}_{3+\delta}$  reveals the formation of a hole-stripe and an orbital fluctuating state in the FMI phase. A Fano antiresonance gives evidence that this is owed to the gain of double-exchange energy in the insulating background. This demonstrates the importance of electronic correlation effects in the manganites.

We thank J. van den Brink, B. Büchner, M. Braden, G. Khaliulin, D. Khomskii, M. Mostovoy and M. M. Savosta for useful discussions. This work was supported in part by the NATO Collaborative Linkage Grant PST.CLG.977766.

<sup>†</sup>To whom correspondence should be addressed. E-mail: [choi@imr.tohoku.ac.jp](mailto:choi@imr.tohoku.ac.jp).

- 
- [1] Y. Tokura and N. Nagaosa, *Science* **288**, 462 (2000).
  - [2] J. v. d. Brink *et al.*, *Colossal Magnetoresistive Manganites*, ed. T. Chatterji, Kluwer Academic Publishers, Dordrecht (2003) and *cond-mat/0206053* (2002).
  - [3] Y. Endoh *et al.*, *Phys. Rev. Lett.* **82**, 4328 (1999).
  - [4] B. Dabrowski *et al.*, *Phys. Rev. B* **60**, 7006 (1999).
  - [5] T. Niemöller *et al.*, *Eur. Phys. J. B* **8**, 5 (1999).
  - [6] Y. Yamada *et al.*, *Phys. Rev. Lett.* **77**, 904 (1996).
  - [7] Y. Yamada *et al.*, *Phys. Rev. B* **62**, 11600 (2000).
  - [8] R. Klingeler *et al.*, *Phys. Rev. B* **65**, 174404 (2002).
  - [9] J. Geck *et al.*, *Phys. Rev. B* **69**, 104413 (2004).
  - [10] J. Geck *et al.*, *New J. Phys.* **6**, 152 (2004).
  - [11] K.-Y. Choi *et al.*, *Phys. Rev. B* **71**, 174402 (2005).
  - [12] T. Mizokawa *et al.*, *Phys. Rev. B* **61**, R3776 (2000).
  - [13] R. Kilian *et al.*, *Phys. Rev. B* **60**, 13458 (1999).
  - [14] W. H. McCarroll *et al.*, *J. Solid State Chem.* **130**, 327 (1997).
  - [15] S. N. Barilo *et al.*, *Physics Solid State* **45**, 146 (2003).
  - [16] C. Ritter *et al.*, *Phys. Rev. B* **56**, 8902 (1997).
  - [17] F. Prado *et al.*, *J. Solid State Chem.* **146**, 418 (1999).
  - [18] K.-Y. Choi *et al.*, *Journ. Phys.: Cond. Mat.* **15**, 3333 (2003) and references therein.
  - [19] Yu. G. Pashkevich *et al.*, *Phys. Rev. Lett.* **84**, 3919 (2000); V. P. Gnezdilov *et al.*, *Low. Temp. Physics* **28**, 510 (2002).
  - [20] K.-Y. Choi *et al.*, *Phys. Rev. B* **71**, in press (2005).
  - [21] R. Krüger *et al.*, *Phys. Rev. Lett.* **92**, 097203 (2004).